Journal of Physics: Conference Series **525** (2014) 012010 doi:10.1088/1742-6596/525/1/012010

Hydrodynamic characterization of a passive shape memory alloy valve

A M Waddell[1], J Punch[1], J Stafford[2,] and N Jeffers[2]

[1] CTVR, Stokes Institute, University of Limerick, Limerick, Ireland
[2] Thermal Management Research Group, Bell Labs, Alcatel-Lucent, Dublin, Ireland

E-mail: alistair.waddell@ul.ie

Abstract. Next generation high-performance electronics will have large heat fluxes (>10^2 W/cm^2) and an alternative approach to traditional air cooling is required. An attractive solution is micro-channel cooling and micro-valves will be required for refined flow control in the supporting micro-fluidic systems. A NiTi Shape Memory Alloy (SMA) micro-valve design was hydrodynamically characterized in this work to obtain the valve loss coefficient (K) from pressure measurements. The hydrodynamic characterization was important as in the flow regime of the micro-fluidic system K is sensitive to Reynolds number (Re) and geometry. Static replicas of the SMA valve geometry were studied for low Reynolds numbers (110 – 220) in a 1x1 mm CSA miniature channel. The loss coefficients were found to be sensitive to flow rate and decreased rapidly with an increase in Re. The SMA valve was compared to a similar gate micro-valve and loss across both valves was of the same order of magnitude. The valve loss coefficients obtained in this work are important parameters in the modeling and design of micro-fluidic cooling systems.

1. Introduction

Electronic devices are constantly evolving towards compact form factors and higher performance. Accompanying this trend is an increase in the heat load (fluxes over 10^2 W/cm^2) that must be dissipated by internal circuitry. Traditional forced convection air cooling methods are reaching their limits and new approaches are required for future devices. A promising approach is the development of an integrated micro-channel cooling system on a chip. A vital component in this micro-fluidic system is a valve structure to control and regulate the flow of coolant.

A normally-closed passive Shape Memory Alloy (SMA) micro-valve design was described in previous work [1] and the developed prototype is shown in figure 1. The valve sits on an Acetal base (1) that slots into the (8x11 mm CSA) miniature-channel test-rig. The main body of the valve and source of obstruction when closed is a 127 μm thick curved stainless steel shim (2). Inserted through the steel shim is a $\varnothing$0.4 mm NiTi actuator wire with an A_f temperature of 40°C. The valve is actuated by the SMA wire's shape memory effect when heated by the flow in the channel. A discussion on the function and response of the working SMA prototype valve is outside the scope of this paper. The focus is instead on the hydrodynamic characteristics of the valve geometry.

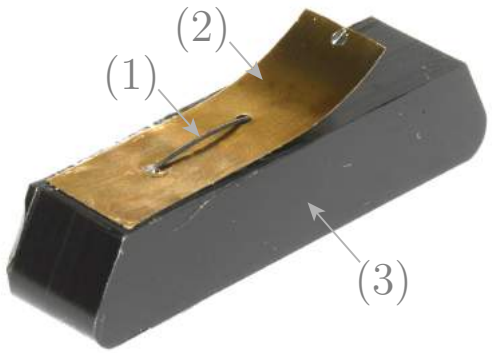

Figure 1. Prototype SMA valve [1]. (1) NiTi actuator wire; (2) stainless steel spring; (3) acetal base.

Figure 2(a) shows an illustration of the closed SMA prototype valve in elevation and end views. Also shown are fluid pathlines around the structure based on flow visualization performed by Waddell *et al.* [1]. On approach to the valve the flow area is gradually reduced. The fluid flows along the perimeter of the valve and subsequently through the two side-orifices in a complex and unsteady motion.

The hydrodynamic characteristics of the SMA valve will be compared with those of a similar gate valve [3]. The gate valve geometry is shown in figure 2(b). It consists of a vertical obstructing wall that occupies a certain fraction of the channel. The flow adjusts around the obstruction accordingly.

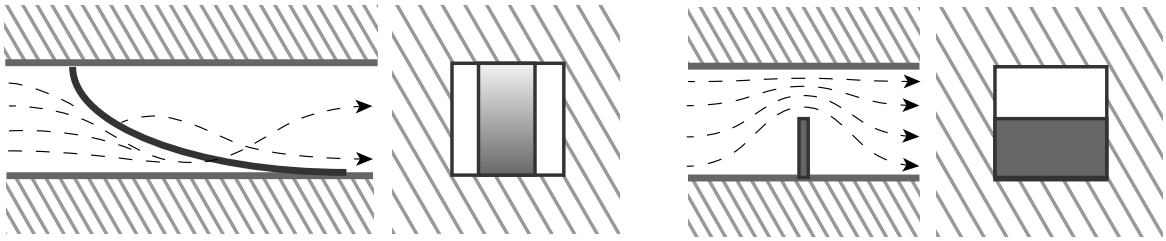

(a) SMA valve (b) Gate valve

Figure 2. Valve geometry in elevation and end view

The head loss coefficient (K) of a valve is an important parameter of the overall system design as the choice of pump must be able to overcome the associated pressure drop. In the turbulent flow regime K is practically constant and independent of Re. For laminar flows (Re $<10^3$), however, K is sensitive to Re and can vary greatly with geometry [2]. For this reason existing correlations could not be used to model the SMA prototype valve and a hydrodynamic characterization study was therefore performed. In the following sections the hydrodynamic characterization experiment on static valve-replicas will be detailed and results presented and discussed.

2. Hydrodynamic characterization method

Static test-pieces replicating the prototype SMA valve geometry were tested and details of these experiments will now be presented.

2.1. Test facility & samples

Reynolds scaling was used to characterize the macro-scale prototype valve geometry in micro-channel like conditions. Characterization was performed on replica geometry of the closed valve

in a 1x1 mm CSA channel. The experimental setup is shown in figure 3. The working fluid (water) and was drawn from a reservoir (1) by a Cole-Parmer gear pump with a micro-fluidic head attachment. The reservoir remained at an ambient temperature of 22±1°C during the tests and the temperature of the flow entering the system was recorded with a K-type thermocouple. After the pump the flow entered the test rig (3) and an Omega PX2300 1 PSI transducer (4) recorded pressure drop across the test section. The transducer output was recorded with a 6009 Ni-DAQmx 14-bit data acquisition card.

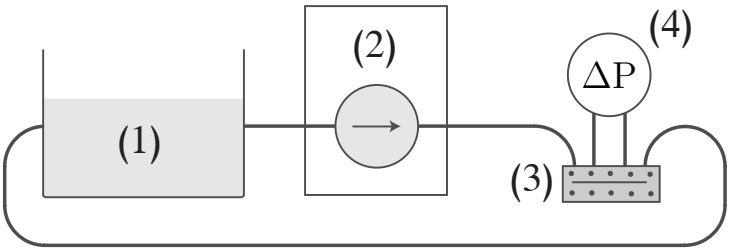

Figure 3. Pressure measurement facility. (1) reservoir; (2) gear pump; (3) test rig; (4) pressure transducer.

The 1 mm miniature channel rig is shown in figure 4. Fluid enters the channel at the inlet (1) and flows across two ⌀0.5 mm pressure taps (2 & 3) before exiting the rig (4). The pressure taps are located one flow development length ($x_{\mathrm{fd}} \approx 0.05Re, Re = 240$) downstream of the inlet and test-section. The test section (5) consists of a slot where different replica valves can be inserted and tested. The test rig consists of an acetal body and polycarbonate window bolted together and sealed with an o-ring (6).

The valve geometry investigated in the current study was determined from the functional experiments involving the SMA valve shown in figure 1. Figure 5 shows a replica of this valve used in the characterization experiments. The sample was constructed from aluminium shim 100μm thick (1), bonded to a 3D-printed base (2) that slotted into the test rig. Six replica valve samples were constructed and had blockage ratios (w/W) ranging from 0.5 to 0.83.

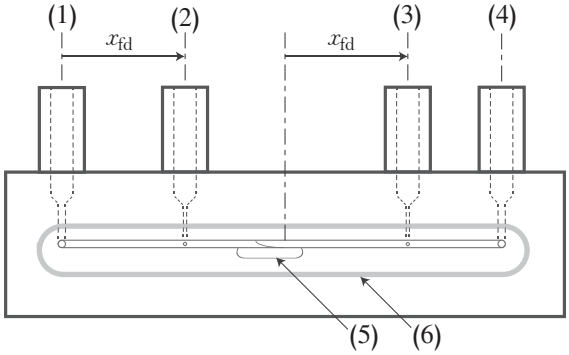

Figure 4. Pressure measurement rig. (1) flow inlet; (2) pressure port 1; (3) pressure port 2; (4) flow outlet; (5) removable test piece; (6) o-ring seal.

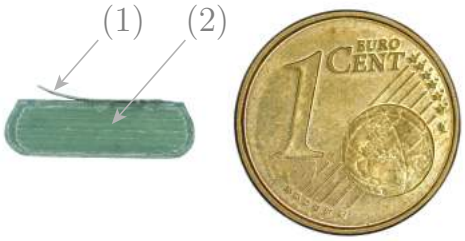

Figure 5. Miniature static valve replica. (1) 100 μm thick aluminium shim; (2) 13 mm long base.

2.2. Method

For each sample the test rig was assembled underwater to remove air, and the bolts were torqued to 5 Nm for consistent compression. The samples were tested over a range of Reynolds numbers

in the channel between 110 and 220. After the system reached steady state for each flow-rate setting 10,000 pressure measurements were recorded and averaged.

3. Data analysis

The primary measurement recorded in the experiments was pressure drop across the test section. The valve loss coefficient (K) was then derived from this data. Analysis was performed on the results by the method of Kline and McClintock to determine the propagation of uncertainty within the results.

3.1. Data reduction

Equation 1 describes pressure-drop in the miniature-channel between the pressure ports. Head loss between two measured points is ΔP, the working fluid density is ρ, mean velocity in the miniature-channel is u, the valve loss coefficient is K, the friction factor f, the distance between the two pressure ports is L and the hydraulic diameter of the miniature-channel is D_h [4].

Head loss in the rig due to friction between the pressure ports was accounted for in the experimental results. Pressure-drop across an empty test section was recorded for the flow rates of interest yielding loss due to friction. These values were then subtracted from pressure-drop measurements across static valves to isolate the head loss contribution from the valve. Rearranging equation 1 for K (the valve loss coefficient) yields equation 2.

$$\Delta P = \frac{1}{2}\rho u^2\left(K + \frac{fL}{D_h}\right) \tag{1}$$

$$K = \frac{2\Delta P}{\rho u^2} \tag{2}$$

3.2. Uncertainty

Potential sources of uncertainty in the pressure measurements included the height-difference between two columns of liquid used in the transducer calibration and the transducer signal noise. A large sample size of 10,000 measurements was recorded and averaged to minimize uncertainty in the signal noise. A Newport optics stage was used to control the differential height between the two columns of water during the calibration. A total uncertainty in the pressure measurements was calculated as ±5.1 Pa by the method of Kline and McClintock [5]. Equation 2 was analyzed to evaluate the uncertainty in the derived variable K. The uncertainties of the primary variables are shown in table 1 and these values were combined by the method of Kline and McClintock, yielding an uncertainty in K that ranged between ± 4.7 and 10.34 %.

Table 1. Experimental uncertainties

Variable	Uncertainty
ΔP	± 5.1 Pa
$\dot{M}$	± 0.043 μL/s
A	± 0.02 mm^2
u	± 2.26 %
K	± 4.7–10.34 %

4. Results & discussion

The hydrodynamic characterization (see section 2) results will now be presented and discussed. Figure 6 shows pressure drop across the 6 samples for a range of flow-rates. Plotted through each data set is a power law curve fit in the form ax^b. All curve fitting constants can be found in table 2. Uncertainty in the data points range from ±1.18 to 9.3 %.

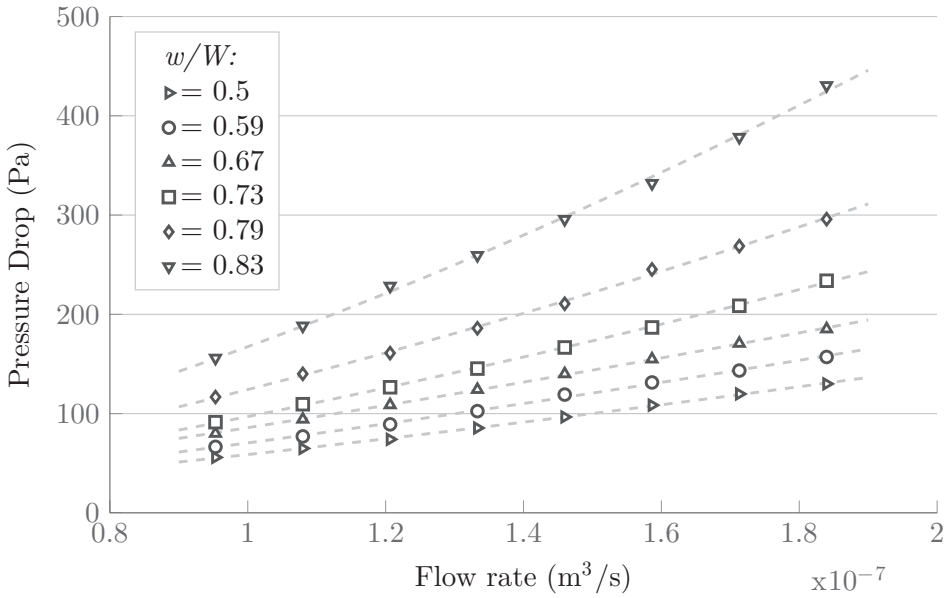

Figure 6. Pressure drop as a function of flow rate for various valve positions.

The data in figure 6 shows the pressure drop increases when w/W is increased and this is to be expected. Further, it can be seen that the pressure drop increases in a non-linear fashion as w/W is increased. More detailed information on the power law curve fits can be found in table 2. The power law exponent increases as w/W is increased, rising from 1.312 to 1.527 in the tests. The curve fits show a strong correlation in the data with an average R^2 of 0.9988.

Table 2. Power law (ax^b) curve fit constants

	ΔP			K		
w/W	a	b	R^2	a	b	R^2
0.5	$8.938\text{x}10^{10}$	1.312	0.9993	290.7	-0.6976	0.9968
0.59	$1.356\text{x}10^{11}$	1.326	0.998	298.3	-0.6662	0.9932
0.67	$6.928\text{x}10^{10}$	1.272	0.9996	450.7	-0.7119	0.9992
0.73	$1.009\text{x}10^{12}$	1.431	0.9995	282.9	-0.5861	0.9979
0.79	$1.29\text{x}10^{12}$	1.431	0.9986	347.6	-0.5781	0.9935
0.83	$8.116\text{x}10^{12}$	1.527	0.998	426.3	-0.5462	0.9915

K as a function of Re for the tested samples is shown in figure 7. Again, a power law curve fit in the form ax^b is plotted through each data set with the curve fitting constants located in table 2. Uncertainty in Re is ± 3.5 %. The uncertainty in K ranges from ± 4.7 to 10.34 %.

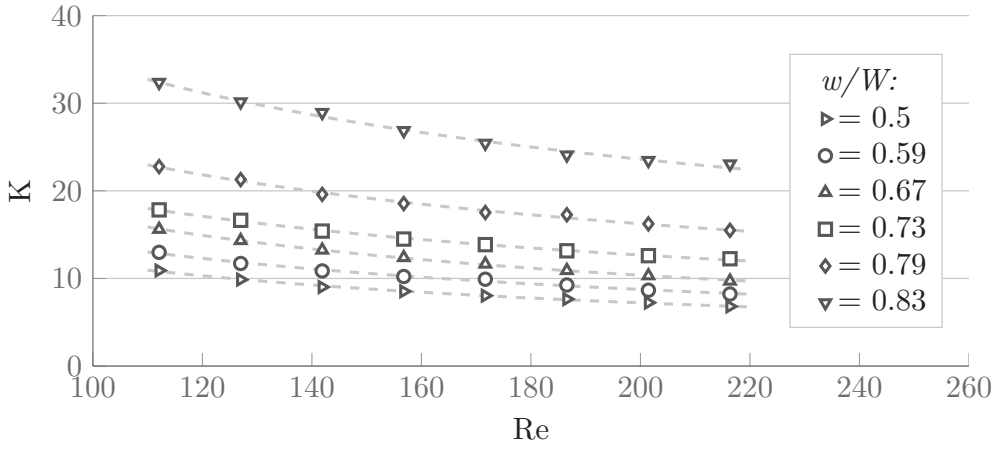

Figure 7. Valve loss coefficient (K) as a function of Re.

As Re is increased K is observed to decrease. The negative exponent of the power law curve fit increases with flow-rate and this implies that K is more sensitive to Re for the greater blockage ratios. For direct comparison with the gate valve (see section 1) characterized by Carretero-Benignos [3] a surface was plotted through the data and used to interpolate values for w/W=0.45. This comparison is plotted on a log-linear graph in figure 8.

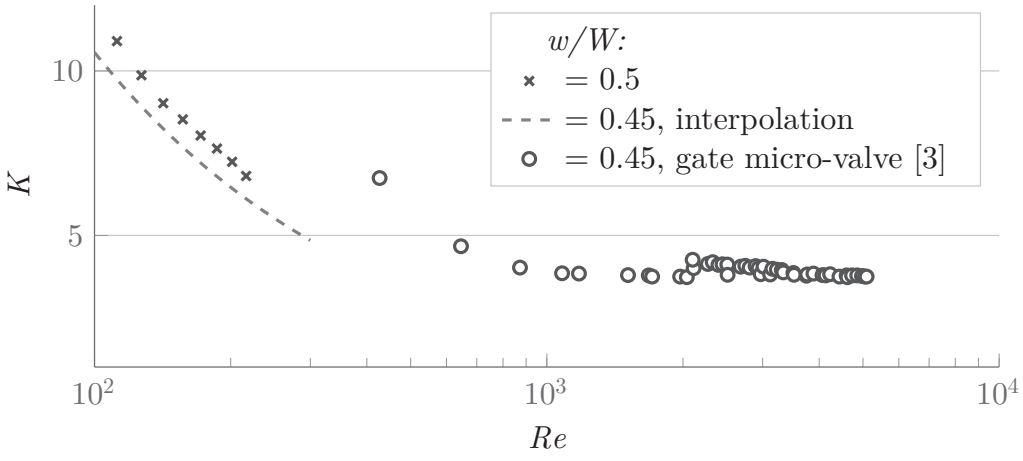

Figure 8. K factors for SMA valve replica compared with gate micro-valve

The K values for both the SMA and gate micro-valves are of the same order magnitude and reduce rapidly as Re is increased. The interpolated SMA valve K-factor curve is offset from the gate valve curve. Consider the geometry of the SMA valve (shown in section 1, figure 2(a)). The valve body is curved and this reduces the flow area gradually. This gradual reduction in area funnels the flow through the two side-orifices. The gate valve (figure 2(b)) consists of a wall perpendicular to the flow that blocks the channel. Unlike the SMA valve there is an abrupt reduction in flow area with no gradual reduction. These disparities in the two valve geometries may explain the difference in K; however the SMA valve has not been tested above Re >220.

In figure 8 K is relatively unaffected by the increase in Re above 10^3. There is a strong dependence as Re is decreased below 10^3 and the loss coefficients for both valves varies by a factor of two. This highlights the importance of understanding the losses associated with micro-scale valves as they operate in this flow regime. In systems incorporating micro-fluidic cooling

the losses across micro-valves will need to be overcome by pumping. As K is sensitive to Re the overall work requirement of the system can vary significantly and needs to be considered in the design. The data presented in this work can be used as a reference in the design and modelling of valve components in future micro-fluidic cooling systems.

5. Conclusions

Hydro-dynamic characterization of a novel SMA micro-valve for application in passive thermal management of high heat flux devices was presented in this work. This analysis was performed on scaled down static replicas of the prototype SMA valve to derive K, the loss coefficient for the valve geometry. Key findings of the work were:

- The valve loss coefficients decrease rapidly with an increase in Re (Re <10^3).
- The valve loss coefficients are lower than those of an equivalent gate valve.

This body of work presents information useful in the design of larger micro-fluidic cooling systems. The head loss curve fit's obtained for the range of experiment parameters can be used to predict the pressure drop across micro-valves in the system and provide a design specification for a micro-pump. Future work will include investigation of the flow structures around the valve and analysis of the heat transfer benefits that can be achieved.

Acknowledgements

The authors acknowledge the financial support of Science Foundation Ireland under grant number 10/CE/I1853. Bell Labs Ireland would like to thank the Industrial Development Agency (IDA) Ireland for their continued support.

Nomenclature

A	Area, miniature-channel	m^2	$\dot{M}$	Mass flow rate	kg/s
A_f	Austenite finish temperature	°C	Re	Reynolds number	-
D_h	Hydraulic diameter	m	u	Velocity	m/s
E	Young's Modulus	GPa	w	Width of valve	m
f	Darcy friction factor	-	W	Width of channel	m
K	Loss coefficient	-	ΔP	Differential pressure	Pa
L	Distance between pressure ports	m	ρ	Density	kg/m^3

References

[1] Waddell A M, Punch J, Stafford J and Jeffers N 2014 *Proc. 7th Int. Heat Transfer Conf. (Kyoto)* (New York: Begell House)
[2] Idelchik I E 1960 *Handbook of Hydraulic Resistance: Coefficients of Local Resistance and of Friction* (Washington: NTIS) p 351
[3] Carretero-Benignos J 2001 *Measurement and Modeling of the Flow Characteristics of Micro Disc Valves* (Massachusetts Institute of Technology: Masters Thesis) p 66
[4] Massey B 2006 *Mechanics of Fluids* (Oxon: Taylor & Francis) pp 245-253
[5] Kline S J and McClintock F A 1953 *Mech Eng.* **75** pp 385-387